

ARTICLES

Infrared absorption study of the hydrogen-bond symmetrization in ice to 110 GPa

K. Aoki, H. Yamawaki, M. Sakashita, and H. Fujihisa

National Institute of Materials and Chemical Research, Tsukuba, Ibaraki 305, Japan

(Received 4 March 1996; revised manuscript received 22 July 1996)

Infrared measurements at room temperature have shown that the hydrogen-bond symmetrization occurs at 62.1 GPa in ice. The OH stretching frequency initially located at 3500 cm^{-1} at ambient pressure falls toward zero around 60 GPa. An absorption band appears in the low-frequency region below 800 cm^{-1} at about 65 GPa, growing a definite peak with a shift to a high frequency by further compression. Such a turn in the pressure dependence of the stretching frequency is an evidence for the transition from ice VII to symmetric ice X. The OH bending peak disappears before the transition. Two absorption peaks, which are originated from the OH stretching and librational vibrations in ice VII, persist above the transition pressure, being assigned to a translational and distortional lattice vibrations in ice X. [S0163-1829(96)00645-5]

INTRODUCTION

The symmetrization of hydrogen bond in ice is intimately related to the quantum motion of protons known as tunneling and has been one of the major subjects in chemistry and physics for over a half century.¹⁻⁶ The energy potential for the proton motion along the hydrogen bonded O-O axis can be described as a double-minimum potential with an energy barrier on the midpoint. As oxygen atoms are pushed closer by applying pressure, the potential barrier will gradually be depressed and eventually the potential may converge into a single minimum at a sufficiently high pressure. Hydrogen-bonded protons initially located at asymmetric positions about one third of the O-O separation⁷ will relocate to the symmetric midpoints (Fig. 1). Water molecules dissociate to form an "atomic crystal" consisting of hydrogen and oxygen atoms, and hence the picture of ice as a molecular crystal breaks down entirely.

The transition into symmetric ice (ice X) has not unambiguously been confirmed in spite of affirmative theoretical results; their predicted transition pressures are below 1 Mbar, attainable pressures with the conventional diamond-anvil cell technique. The microscopic transition mechanism has been investigated previously using semiempirical methods¹⁻⁴ and very recently using *ab initio* quantum-mechanical methods.^{5,6} Starting from a proton-ordered structure of ice VIII, they calculated the transition pressures into ice X ranging from 35 to 80 GPa. These predicted pressures can immediately be applied to the symmetrization in ice VII without major corrections. Ice VII has a crystal structure very close to that of ice VIII; a body-centered-cubic (bcc) lattice of oxygen atoms with disordered protons. A number of high-pressure experiments have been made to explore the symmetric ice and several of them reported some indications of phase transitions in both ice VII and VIII at about 50 GPa, which were interpreted in relation to the hydrogen-bond symmetrization. It was an anomaly in the Brillouin frequency of ice VII (Ref. 8) or the appearance of a lattice

vibrational peak in the Raman spectra of ice VIII.^{9,10} Very careful Raman measurements, however, revealed recently that the phase transitions associated with the hydrogen-bond symmetrization did not take place either in ice VII at room temperature or in ice VIII at low temperature.^{11,12}

The structural study of ice by x-ray diffraction has provided hopeful results on the hydrogen-bond symmetrization, although the obtained structural information was limited to the compression of the oxygen lattice. The bcc lattice of oxygen atoms in phase VII was found to exist over a very wide pressure range at least to 128 GPa. At this pressure the O-O distance along the hydrogen bonding decreases to 0.228 nm.¹³ This value is sufficiently less than 0.24–0.25 nm of the threshold distances theoretically predicted¹⁻⁶ for the symmetrization transition and slightly shorter than the O-O distances in some molecular crystals in which the hydrogen-bond symmetrization is realized at ambient pressure.¹⁴ High-pressure x-ray-diffraction data, hence, leads to a plausible and realistic idea that the symmetrization would already take

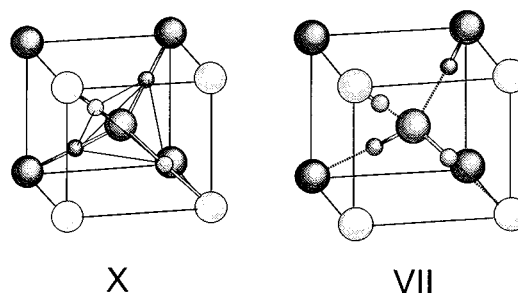


FIG. 1. The crystal structures of symmetric ice (ice X). The corresponding unit cut out from the cubic unit cell of ice VII is also presented for comparison. The ice VII structure can be converted into the ice X structure simply by displacing the hydrogen atoms to the midpoints along the hydrogen bonding. In ice X, four first neighboring hydrogen atoms form a tetrahedron with one oxygen atom at the center.

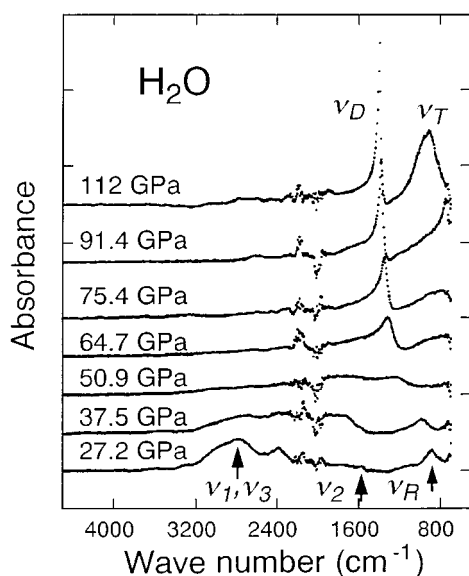


FIG. 2. Infrared absorption spectra of ice measured with KBr medium. Three infraactive intramolecular vibrations, a symmetric bond stretching (ν_1), an asymmetric bond stretching (ν_3), and a bond bending vibration (ν_2), were observed. In addition, one librational vibration (ν_R) began to appear at above 10 GPa. At pressures above 90 GPa, two peaks located at about 1000 and 1400 cm^{-1} were clearly observed; they were assigned to a translational (ν_T) and distortional (ν_D) lattice modes in ice X. Large noises ranging from 2000 to 2400 cm^{-1} were due to incomplete cancellation of the strong absorption of the diamond anvils in background subtraction procedures.

place in ice VII with keeping its bcc lattice in the pressure range explored.

Infrared absorption spectroscopy is one promising method to investigate the hydrogen-bond symmetrization in ice. The water molecule has three fundamental vibrations: the symmetric and asymmetric OH stretching vibrations, respectively, ν_1 and ν_3 , and the OH bending vibration, ν_2 .¹⁵ In molecular solids all of these vibrational modes are both infrared and Raman active, and their pressure behaviors can fundamentally be investigated by either spectroscopy. This biactivity in the vibrational motions should be altered in association with the transition into symmetric ice. These three molecular vibrations are converged into two lattice vibrational modes, one distortional twisting motion of hydrogen atoms (ν_D) and one translational motion of coupled oxygen and hydrogen atoms (ν_T), and both vibrational modes are not Raman active but infrared active.^{10,16} Infrared absorption measurement is expected to give a more clear insight into the hydrogen-bond symmetrization. Some infrared measurements of ice have been made, reporting the pressure dependence of the fundamental and combination bands. The measured pressure range, however, has been limited to 20 GPa,^{15,17} and recently has been extended to 40 GPa,¹⁸ still below the expected symmetrization pressures. In this paper the infrared measurement of ice beyond 100 GPa will be presented.

EXPERIMENTAL

High-pressure infrared spectra were measured with a piston-cylinder type diamond-anvil cell (DAC).¹⁹ Because of

very strong absorption from ice, preparation of thin films in the DAC was required to obtain unsaturated spectra available for quantitative analysis of the spectral profile. The disconnected piston and cylinder of the DAC were cooled with liquid nitrogen in a glove chamber purged with dry nitrogen gas. Ice films were prepared by condensation of evaporated water on the top surface of one diamond anvil with a fixed metal gasket, and successively the gasket hole was filled with pressure transmitting medium. The DAC was quickly assembled and was left in the glove box for a few hours until warming up to room temperature. Xenon (Xe), potassium bromide (KBr), and tetrachloromethane (CCl_4) were used as pressure media. The former two are transparent over the whole wave-number region measured, while the latter is transparent above 1000 cm^{-1} . The water molecule shows the absorption peaks associated with the molecular vibrations at the high-frequency region above 1000 cm^{-1} at modest pressures and hence the spectrum is not significantly disturbed by absorption from a pressure medium of CCl_4 , in particular, at relatively low pressures.

The diamond anvils used were type II-A with a beveled cut shape. The culet diameter was 0.1 mm and thickness was 1.5 mm. Although diamond itself has strong absorption in the wave-number region of 2200 – 2400 cm^{-1} , such thin anvils allowed transmission by a few percent of incident lights and hence collection of the overall spectral profile. The initial thickness of an indented metal gasket was about 25 μm . The sample hole with an initial diameter of 30 μm , which was made on the gasket with an electric discharge machine, was enlarged to 50 – 60 μm in diameter during compression. Transmitting lights were collected through an optical mask typically with a passing area of 25×25 μm^2 in order to reduce degradation of spectra due to the pressure gradient in the specimen. A microscope Fourier transform infrared spectrometer covering the wave-number region from 700 to 5000 cm^{-1} was used with a spectral resolution of 4 cm^{-1} . Pressure was determined on the basis of the ruby fluorescence scale.²⁰

SPECTRAL CHANGE AND ANALYSIS

Absorption spectra of ice VII were collected with Xe medium to 86 GPa, KBr to 112 GPa, and CCl_4 to 107 GPa. These experiments provided the consistent results each other and ruled out possibility of the formation of chemical compounds between ice and the pressure media. Typical spectra of ice pressurized in KBr are shown in Fig. 2. The symmetric and asymmetric stretching peaks overlapped entirely to form an inseparable broadened peak. The central position of the overlapped peaks shifts from about 2840 to 1700 cm^{-1} , while the pressure increases from 27.2 to 50.9 GPa. The peak shift is accompanied with an enormous peak broadening. An absorption band appears in the low-frequency region around 800 cm^{-1} at 64.7 GPa (see Fig. 3), growing a definite peak on further compression. As described in detail later, the transition from ice VII to X was observed at 62.1 GPa. Two absorption peaks clearly seen at about 1400 and 1000 cm^{-1} in the top spectrum measured at 112 GPa were hence assigned to distortional and translational lattice modes in ice X. The asymmetrically deformed librational peak gets sharp at pressures above 64.7 GPa, while the OH bending vibrational peak, which stays at nearly the same position of 1550 cm^{-1} , disappears below 50 GPa.

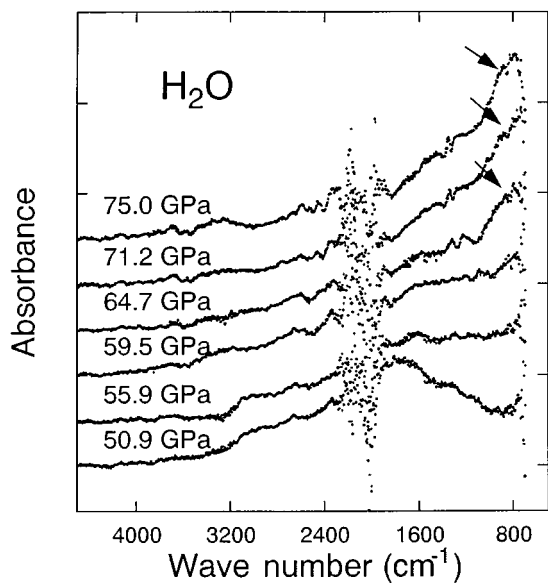


FIG. 3. Spectral change associated with the hydrogen-bond symmetrization. An asymmetrically deformed peak of the librational vibration was subtracted from a raw spectrum using fitted Fano parameters. An absorption band appears in the frequency region around 800 cm^{-1} at 64.7 GPa, showing a peak shift to a high frequency with increasing pressure.

Broadening and asymmetric deformation in absorption peak make it difficult to determine correctly the central position of the stretching peak from the raw spectra. The unperturbed spectral features of the stretching mode can be extracted by subtracting an interfered peak shape fitted with

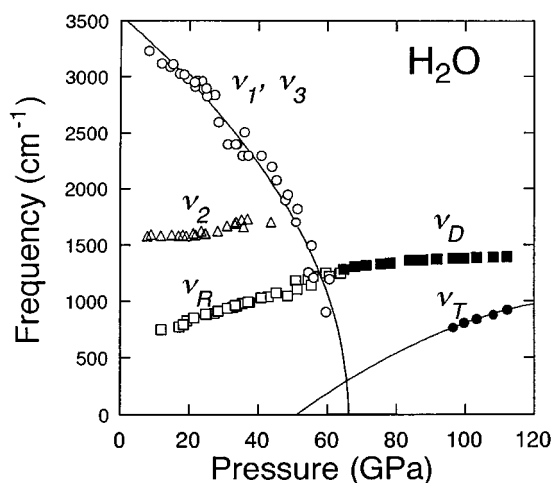


FIG. 4. The observed peak frequencies are plotted as a function of pressure. The OH stretching frequencies (ν_1 and ν_3) fall towards zero at about 60 GPa. The new peak (ν_T), which might appear below 700 cm^{-1} just after the transition, shows a shift to a high frequency with pressure. The OH bending frequency (ν_2), showing a pressure insensitive behavior, disappears at about 45 GPa. The librational (ν_R) and distortional lattice (ν_D) modes show a monotonic increase in frequency over the entire pressure region without discontinuous change but with a change in slope at the transition pressure.

a Fano function^{21,22} from an original spectrum. An interfered peak shape is described with a function of frequency as

$$I \propto (q + \epsilon)^2 / (1 + \epsilon^2),$$

where q is a line-shape parameter and ϵ is a normalized energy given by $(\omega - \omega_0)/\Gamma$: ω_0 is an unperturbed frequency and Γ is a linewidth parameter. Figure 3 shows the absorption spectra obtained by this spectral processing. The absorption peak, which is located at 1700 cm^{-1} in the spectrum measured at 50.9 GPa, collapses to an enormously broadened peak by further compression. The peak position for such a collapsed peak was estimated from a peak-profile fitting with a given peak width under the assumption of a Lorentzian shape. The calculated peak positions were, for example, 1200 and 900 cm^{-1} for the spectra measured at 55.9 and 59.5 GPa, respectively.

A remarkable change in spectral profile is observed at 64.7 GPa. An absorption band appears in the low-frequency region around 800 cm^{-1} , showing a gradual increase in intensity and a shift to a high frequency with increasing pressure. It becomes a well-defined peak shape above 100 GPa as already shown in Fig. 2. The spectral change suggests a phase transition at pressures between 59.5 and 64.7 GPa likely in association with the hydrogen-bond symmetrization. The observed peak shifts with pressure are plotted in Fig. 4. The OH stretching frequency (ν_1 and ν_3) decreases at an initial rate of $-30\text{ cm}^{-1}/\text{GPa}$, intersecting the bending and librational frequencies, respectively, at about 48 and 56 GPa. Around 60 GPa the stretching frequency goes below the measuring limit of 700 cm^{-1} . By fitting the observed frequencies with a phenomenological function, $\omega = (\omega_0^2 - ap)^{1/2}$, ω_0 (the frequency at ambient pressure) and a (the pressure coefficient) were obtained to be 3549 cm^{-1} and $1.91 \times 10^4\text{ cm}^{-2}/\text{GPa}$, respectively. The frequencies (ν_T) alternatively measured in the high-pressure region above 90 GPa were fitted with a quadratic form, giving $\omega = -1411 + 33.5p - 0.113p^2$. The OH bending frequency (ν_2) shows pressure-insensitive behavior. A slight increase above 30 GPa is probably attributed to asymmetric deformation in the peak shape. The bending frequencies plotted were obtained from the apparent peak maxima of the interfered peaks, which were shown to be pushed slightly toward a high frequency.²² The librational frequency (ν_R) shows a monotonic increase from 830 to 1260 cm^{-1} as the pressure increases from 20 to 60 GPa. The variation of the frequency becomes small after the conversion to the distortional lattice mode at 62 GPa.

The width γ and line-shape parameter q , which were obtained for the asymmetrically deformed librational peaks, are plotted as a function of pressure along with those of the uninterfered peaks obtained by fitting with a Lorentzian function (Fig. 5). Thus obtained γ shows a monotonic decrease with pressure from 180 cm^{-1} at 2 GPa to 20 cm^{-1} at 100 GPa. In contrast, q increases with pressure and its values seem to be divided into two regions below 1.5 and above 2.0. An increase in q indicates that the asymmetric librational peak changes gradually into a symmetric peak. At the limit of $1/q=0$ the interference effect vanishes and the asymmetrically deformed peak shape converges into a symmetric Lorentzian shape. This tendency can be seen in Fig. 2, although the asymmetric shape still remains at 112 GPa. Ad-

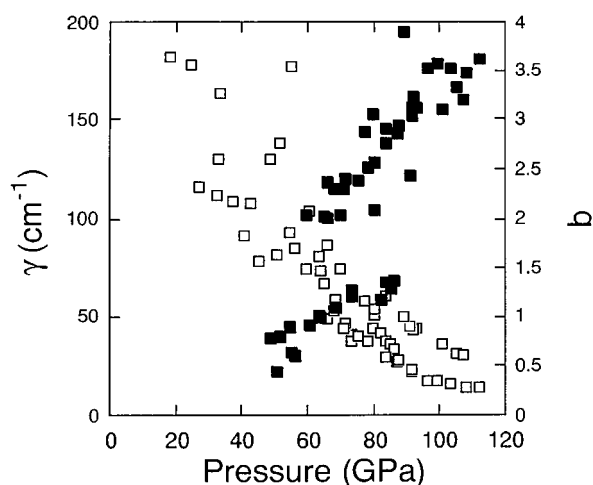


FIG. 5. Pressure variations of the peak width γ (open squares) and peak shape parameter q (closed circles). The gradual decrease in γ represents sharpening of the absorption peak with pressure, while the increase in q shows a successive approach to a symmetric peak shape.

ditional several tens of gigapascals may be required beyond 100 GPa for complete removal of the asymmetric shape.

PHASE TRANSITION AND HYDROGEN-BOND SYMMETRIZATION

The observed infrared spectra show that a phase transition takes place at about 62 GPa and this transition is associated with the hydrogen-bond symmetrization. The phase transition was detected as a turn in the pressure dependence of the stretching frequency. The frequency decreases sublinearly with increasing pressure, falling toward zero around 60 GPa. The turn to an increase in the stretching frequency is not evidently observed in the spectra because of the peak broadening and the limit of low-frequency region measured. However, the appearance of the peak and its shift to a high frequency with pressure indicates unambiguously a phase transition to symmetric ice at a pressure between 59.5 and 64.7 GPa. We adopt here the midpoint of the two pressures, that is, 62.1 GPa. The transition pressure can also be estimated as an intersecting point between the fitted curves for the OH stretching and translational lattice modes. This leads to a slightly high pressure of 65 GPa. The transition pressure of 62.1 GPa is lower by 10 GPa than that previously estimated from Raman frequencies measured for a relatively narrow pressure range to 25 GPa.¹²

Disappearance of the OH bending peak is another spectral feature indicating occurrence of the hydrogen-bond symmetrization. This peak shows a gradual decrease in intensity with pressure and eventually disappears below 50 GPa. The peak-vanishing pressure was not exactly determined from the observed spectra owing to the very weak peak intensity. It should be noted that the bending peak once disappeared was not observed again after the transition. If the bending peak recovered the absorption intensity at higher pressures, it should appear at a frequency close to 1500 cm^{-1} . As seen in the spectrum measured at 112 GPa in Fig. 2, the third peak was not observed. The phase transition is thus accompanied

by disappearance of the OH bending peak. In contrast to the bending peak disappearing, the two absorption peaks originally associated with the OH stretching and molecular rotational vibrations are shown to exist over the whole pressure region measured.

The vibrational mode analysis has predicted only two infrared-active lattice modes for symmetric ice.^{10,16} One is a translational vibration associated with opposite displacements of hydrogen and oxygen atoms and the other is a rhombohedral distortion of the tetrahedron of hydrogen atoms with one oxygen atom at the center (see Fig. 1). The former corresponds to the OH stretching vibration in the molecular phase, while the latter is related to the OH bending and the molecular rotational vibrations which converge into one degenerated lattice mode at the transition point. Only two peaks were observed in the spectra measured above 100 GPa, in agreement with the results of the vibrational mode analysis. The peaks located at about 1400 and 1000 cm^{-1} are consequently assigned to the distortional (ν_D) and translational (ν_T) vibrational modes in ice X, respectively.

The transition pressure determined from the present infrared measurement is in good agreement with that obtained from the analysis of the equation of state for ice. The volume compression data obtained by x-ray diffraction was analyzed in detail using a universal equation of state, and was found to be divided into three regions with two phase transitions at 40 and 70 GPa.²³ The lower transition was related to the hydrogen-bond symmetrization and the higher one to a phase transition on the basis of previously reported Raman and Brillouin data.⁸⁻¹⁰ The change in the equation of state at 40 GPa is so small that it might be ignored, but that at 70 GPa is much more significant and distinct. If we took the present infrared results into account, it is apparently reasonable to attribute the phase transition at 70 GPa rather than that at 40 GPa to the hydrogen-bond symmetrization. A very recent x-ray-diffraction measurement of ice VII confirmed a similar anomaly in the equation of state at 66 GPa,²⁴ again in good agreement with the present infrared results.

It is interesting to examine the hydrogen-bond symmetrization from the viewpoint of the crystal structure. From the x-ray-diffraction data, the hydrogen-bonded O-O distance at 62.1 GPa is calculated to be 0.240 nm; the symmetrized OH distance is 0.120 nm. These values are very close to those of theoretical calculations predicting the symmetrization at the threshold O-O distances of 0.23–0.24 nm. A recent neutron-diffraction study of ice VIII, which is a proton-ordered phase derived from a slight distortion of the bcc lattice of ice VII, revealed a very small pressure dependence of the OD bonding, $4 \times 10^{-5}\text{ nm/GPa}$.²⁵ If we adopted the same pressure dependence for ice VII with an initial OH distance of 0.099 nm, the OH distance would extend by about 18% at the transition pressure of 62.1 GPa. Such an abrupt extension should produce some kinds of discontinuous change in vibrational property, in particular, in the OH stretching vibration. This does not agree with what is actually observed in the present infrared measurement. The latest calculation of the hydrogen bonding in ice shows that the OH bonding distance increases superlinearly as a result of potential deformation, being accelerated at higher pressures.²⁶ In such a case a continuous relocation of protons to the symmetric positions may take place. A second-order-like nature still remains for the

hydrogen-bond symmetrization.

The theoretical study of the hydrogen-bond symmetrization in ice has predicted an order-disorder transition prior to the symmetrization.⁴ This transition is characterized as appearance of a proton-disordered structure in which protons occupy equally the two minima of the double-well potential along the hydrogen-bonded oxygen-oxygen axis. In such a disordered structure water molecules still persist. This is in

contrast to symmetric ice where the molecules dissociate as illustrated in Fig. 1. The remarkable change in spectrum suggesting a transition to the disordered phase was not observed in the present study. The disordered phase may exist for a narrow pressure range as theoretically predicted.⁴ Low-temperature infrared measurements are required to explore the order-disorder transition and clarify the transition mechanism in relation to the hydrogen-bond symmetrization.

-
- ¹C. Reid, *J. Chem. Phys.* **30**, 182 (1959).
²W. B. Holzapfel, *J. Chem. Phys.* **56**, 712 (1972).
³F. H. Stillinger and K. S. Schweizer, *J. Phys. Chem.* **87**, 4281 (1983).
⁴K. S. Schweizer and F. H. Stillinger, *J. Chem. Phys.* **80**, 1230 (1984).
⁵C. Lee, D. Vanderbilt, K. Laasonen, R. Car, and M. Parrinello, *Phys. Rev. Lett.* **69**, 462 (1992).
⁶C. Lee, D. Vanderbilt, K. Laasonen, R. Car, and M. Parrinello, *Phys. Rev. B* **47**, 4863 (1993).
⁷J. D. Jorgensen and T. G. Worlton, *J. Chem. Phys.* **83**, 329 (1985).
⁸A. Polian and M. Grimsditch, *Phys. Rev. Lett.* **52**, 312 (1984).
⁹K. R. Hirsh and W. B. Holzapfel, *Phys. Lett.* **101A**, 142 (1984).
¹⁰K. R. Hirsh and W. B. Holzapfel, *J. Chem. Phys.* **84**, 2771 (1986).
¹¹Ph. Pruzan, J. C. Chervin, and B. Canny, *J. Chem. Phys.* **99**, 9842 (1993).
¹²Ph. Pruzan, *J. Mol. Struct.* **322**, 279 (1994).
¹³R. J. Hemley, A. P. Jephcoat, H. K. Mao, C. S. Zha, L. W. Finger, and D. E. Cox, *Nature (London)* **330**, 734 (1987).
¹⁴M. Ichikawa, *Acta Crystallogr. Sect. B* **34**, 2704 (1978).
¹⁵W. B. Holzapfel, B. Seiler, and M. Nicol, *J. Geophys. Res.* **89**, B707 (1984).
¹⁶K. H. Huang, *Z. Phys.* **171**, 213 (1963).
¹⁷D. D. Klug and E. Whalley, *J. Chem. Phys.* **81**, 1220 (1984).
¹⁸K. Aoki, H. Yamawaki, and M. Sakashita, *Science* **268**, 1322 (1995).
¹⁹K. Aoki, Y. Kakudate, M. Yoshida, S. Usuba, K. Tanaka, and S. Fujiwara, *Jpn. J. Appl. Phys.* **26**, 2107 (1987).
²⁰H. K. Mao, P. M. Bell, J. W. Shaner, and D. J. Steinberg, *J. Appl. Phys.* **49**, 3276 (1978).
²¹U. Fano, *Phys. Rev.* **124**, 1866 (1961).
²²K. Aoki, H. Yamawaki, and M. Sakashita, *Phys. Rev. Lett.* **76**, 784 (1996).
²³J. Hama and K. Suito, *Phys. Lett. A* **187**, 346 (1994).
²⁴E. Wolanin, Ph. Pruzan, M. Gauthier, J. C. Chervin, B. Canny, M. Hanland, and D. Häuserman (private communication).
²⁵R. J. Nelmes, J. S. Loveday, R. M. Wilson, J. M. Besson, Ph. Pruzan, S. Klotz, G. Hamel, and S. Hull, *Phys. Rev. Lett.* **71**, 1192 (1993).
²⁶L. Ojamäe, K. Hermansson, R. Dovesi, C. Roetti, and V. R. Saunders, *J. Chem. Phys.* **100**, 2128 (1994).